Electronic Supplementary Material (ESI) for Nanoscale.

Reconfigurable chirality with achiral excitonic materials in the strong-coupling regime

Electronic Supporting Information

P. Elli Stamatopoulou,[1] Sotiris Droulias,[2] Guillermo P. Acuna,[3] N. Asger Mortensen,[1,4] and Christos Tserkezis[1]

[1] *Center for Nano Optics, University of Southern Denmark, Campusvej 55, DK-5230 Odense M, Denmark**

[2] *Department of Digital Systems, University of Piraeus, GR-18534, Piraeus, Greece*

[3] *Department of Physics, University of Fribourg, Chemin du Musée 3, Fribourg CH-1700, Switzerland*

[4] *Danish Institute for Advanced Study, University of Southern Denmark, Campusvej 55, DK-5230 Odense M, Denmark*

* elli@mci.sdu.dk

Analytic expression for chirality density

The local chirality density for L/RCP waves of frequency ω in a medium characterized by permittivity ε and permeability μ is given by the expression

$$C(\mathbf{r},\omega) = -\frac{\omega}{2}\mathrm{Im}\Big\{\mathbf{D}^*(\mathbf{r},\omega)\cdot\mathbf{B}(\mathbf{r},\omega)\Big\} = -\frac{\omega}{2c^2}\mathrm{Im}\Big\{(\varepsilon^*\mu)\,\mathbf{E}^*(\mathbf{r},\omega)\cdot\mathbf{H}(\mathbf{r},\omega)\Big\}, \tag{S.1}$$

where $\mathbf{E}$ is the electric field, $\mathbf{B}$ the magnetic induction, $\mathbf{D}$ the displacement field, $\mathbf{H}$ the magnetic field and c the speed of light in vaccum. In Fig. 1(c) of the main text we calculate the chirality density inside an achiral high-index dielectric nanoparticle (NP) of radius R, integrated over the volume of the particle

$$\mathcal{C}(\omega) = \int_0^R dr r^2 \int d\Omega\, C(\mathbf{r},\omega) = -\frac{\omega}{2c^2}\mathrm{Im}\Big\{(\varepsilon^*\mu)\int dr r^2\int d\Omega\,\mathbf{E}^*(\mathbf{r},\omega)\cdot\mathbf{H}(\mathbf{r},\omega)\Big\}, \tag{S.2}$$

with $d\Omega$ denoting the differential solid angle. The fields inside the NP can be expressed in terms of vector spherical harmonics $\mathbf{X}_{lm}(\theta,\phi)$ [1]

$$\mathbf{E}(\mathbf{r},\omega) = \sum_{lm}\Big[a^H_{lm} j_l(kr)\mathbf{X}_{lm}(\theta,\phi) + \frac{i}{k}a^E_{lm}\nabla\times j_l(kr)\mathbf{X}_{lm}(\theta,\phi)\Big] \tag{S.3a}$$

$$\mathbf{H}(\mathbf{r},\omega) = \frac{1}{Z}\sum_{lm}\Big[a^E_{lm} j_l(kr)\mathbf{X}_{lm}(\theta,\phi) - \frac{i}{k}a^H_{lm}\nabla\times j_l(kr)\mathbf{X}_{lm}(\theta,\phi)\Big], \tag{S.3b}$$

where l, m are the angular momentum indices, $k = \omega/c\sqrt{\varepsilon\mu}$ is the wavenumber and $Z = \sqrt{\mu\mu_0/(\varepsilon\varepsilon_0)}$ the impedance in the medium, j_l is the spherical Bessel function of the first kind and $a^{E/H}_{lm}$ are expansion coefficients that can be found by solving the boundary conditions of the problem, as in standard Mie theory [2]. Substitution of eqn (S.3) in eqn (S.2) gives

$$\mathcal{C}(\omega) = -\frac{\omega}{2c^2}\sum_{lm}\mathrm{Im}\Big\{\frac{\varepsilon^*\mu}{Z}\Big[a^{H*}_{lm}a^E_{lm}\mathcal{I}^1_{lm} - a^{E*}_{lm}a^H_{lm}\mathcal{I}^2_{lm}\Big]\Big\}, \tag{S.4}$$

with

$$\mathcal{I}^1_{lm} = \int_0^R dr r^2\big|j_l(kr)\big|^2 \tag{S.5a}$$

$$\mathcal{I}^2_{lm} = \frac{1}{|k|^2}\Big\{\int_0^R dr\, l(l+1)\big|j_l(kr)\big|^2 + \big|Rj_l(kR)\big|^2\Big\}. \tag{S.5b}$$

In Figs. 1(c), 2(e) and (f) of the main text, we normalize the chirality density to its value for L/RCP waves in bulk media, where $\mathbf{H}_{\mathrm{L/R}} = \mp i\mathbf{E}_{\mathrm{L/R}}/Z$, therefore

$$C^{L/R}_{\mathrm{bulk}}(\mathbf{r},\omega) = \pm\frac{\omega}{2c^2}\mathrm{Re}\Big\{\frac{\varepsilon^*\mu}{Z}\Big\}. \tag{S.6}$$

For the volume-averaged values $\mathcal{C}^{L/R}_{\mathrm{bulk}}(\omega)$ one need simply multiply with the volume of the NP.

Differential Scattering (DS) and Circular Dichroism (CD)

Fig. S.1 shows the DS and CD spectra for an uncoated chiral sphere of radius $R = 85$ nm. and permittivity $\varepsilon = 12.1 + 0.001i$ in air. For a real-valued $\kappa = 0.001$, the CD signal [Fig. S.1(c)] is very low, of the order of 10^{-5}, that is two orders of magnitude lower than DS [Fig. S.1(a)]. Comparison with Fig. 3(c) of the main text, which shows the CD of the coupled chiral sphere, provides evidence that the excitonic material can increase the CD signal by two orders of magnitude, due to its resonant nature, even though it is itself achiral.

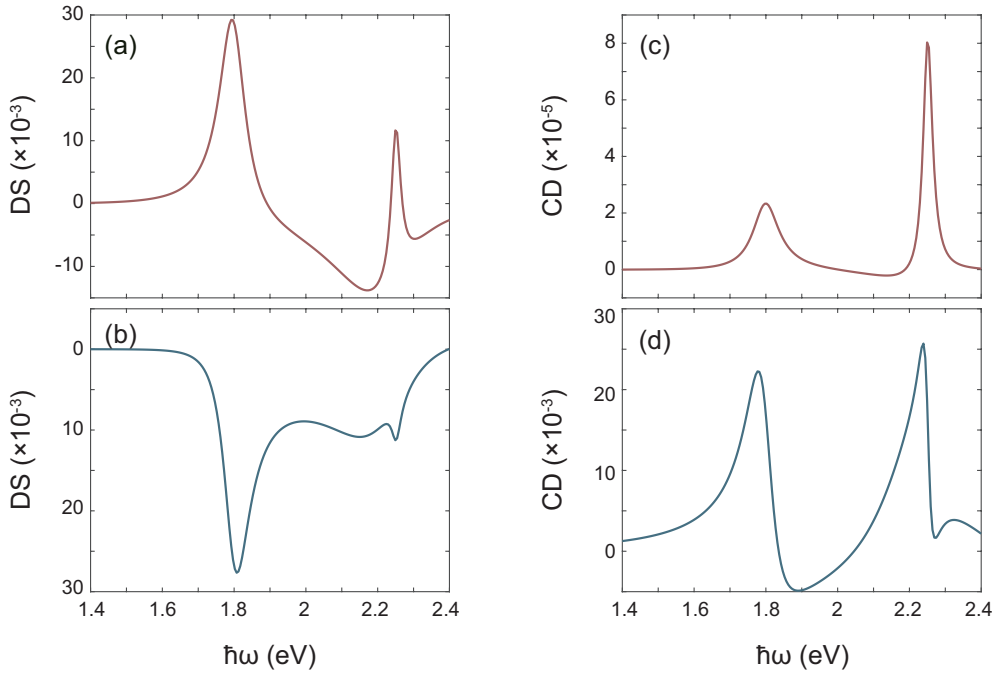

FIG. S.1. (a-b) Differential scattering (DS) and (c-d) circular dichroism (CD) spectra of an uncoated chiral NP of radius $R = 85$ nm and permittivity $\varepsilon = 12.1 + 0.001i$ for a real Pasteur parameter $\kappa = 0.001$ (a,c), and for an imaginary $\kappa = 0.001i$ (b,d) .

On the other hand, an imaginary-valued $\kappa = 0.001i$ produces a higher CD signal [Fig. S.1(d)], of the same order of magnitude as the DS spectrum of the same structure [Fig. S.1(b)]. In this case, as shown in Fig. 3(d) in the main text, the excitonic shell leads to the splitting of the resonant feature, here the magnetic dipolar (MD) mode, when operating within the strong coupling regime. Excitonic materials can thus be employed either to enhance the chiroptical response of a nanostructure or to quantitatively reconfigure spectral features. The splitting itself can be tailored through the optical characteristics of the exci-

tonic material. For example, Fig. S.2 shows the widening of the splitting in both DS and CD spectra of the chiral sphere with real-valued $\kappa = 0.001$, as the oscillator strength of the excitonic shell increases.

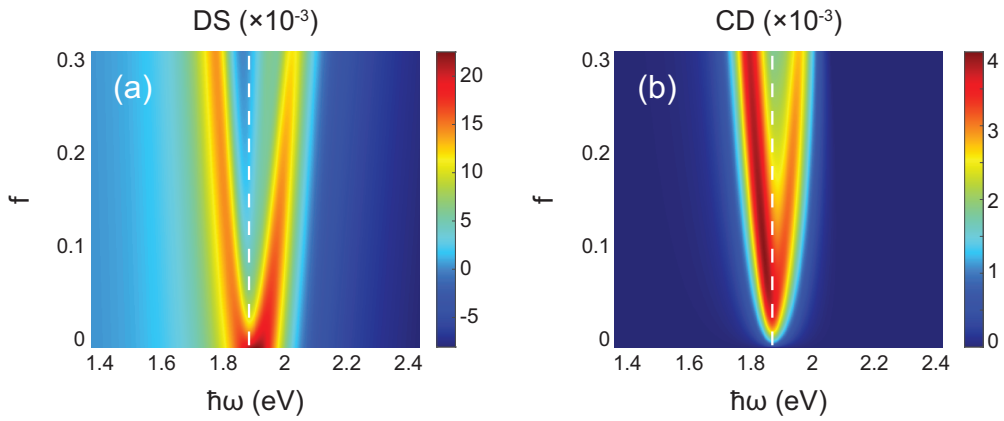

FIG. S.2. (a) DS and (b) CD spectra of the chiral ($\kappa = 0.001$) NP coated with the excitonic shell tuned at transition energy $\hbar\omega_{\text{exc}} = 1.88$ eV as a function of the oscillator strength f. Dashed white lines serve as guides to the eye for tracing the energy of the excitonic resonance.

Strong coupling study

To confirm that the coupled NP studied in the main text operates in the strong coupling regime we examine the standard criterion that the coupling strength g, which is proportional to the splitting of the MD mode, is larger than a critical value determined by the damping rates of the two resonant systems individually [3]. This condition quantifies as

$$2g > \sqrt{\frac{\gamma_{\text{exc}}^2 + \gamma_{\text{MD}}^2}{2}}. \tag{S.7}$$

To determine the damping rate of the MD mode of the uncoupled NP, we fit the contribution as calculated by Mie theory with a sum of two Lorentzian curves to account for the asymmetry of the mode. This asymmetry is owed to contributions of higher radial order modes which are captured by the broad Lorentz curve illustrated with a green line in Fig. S.3(a). The damping rate of the MD mode that couples to the excitonic resonance corresponds to the linewidth of the Lorentzian curve centered at around 2 eV, which we find to be $\hbar\gamma_{\text{MD}} = 0.15$ eV.

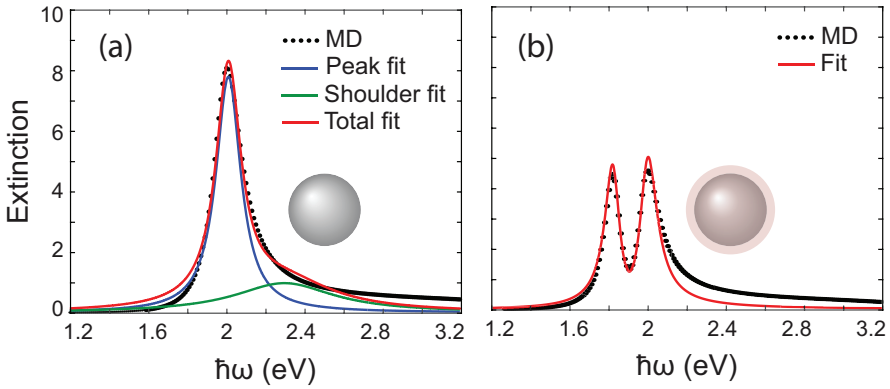

FIG. S.3. (a) The magnetic dipolar contribution to extinction cross section of the uncoated achiral NP of radius $R = 85$ nm and permittivity $\varepsilon = 12.1 + 0.001i$ (black circles) is fitted by the sum of the two Lorentzian lineshapes (blue and green line). The total fit (red line) reproduces well the linewidth of the magnetic dipole. (b) The magnetic dipolar contribution to extinction cross section of the same NP as in (a), coated with an excitonic shell of transition energy $\hbar\omega_{\rm exc} = 1.88$ eV, damping $\hbar\gamma_{\rm exc} = 0.05$ eV, oscillator strength $f = 0.2$ and background permittivity $\varepsilon_b = 3$ (black circles). The coupling strength of the two-layered NP is extracted by fitting with a system of two coupled harmonic oscillators (red line).

The coupled system can be described by a two-coupled-oscillators model. The equations of motion of the bound charges in the NP and the excitons in the excitonic shell are given by the system

$$\ddot{x}_{\rm MD}(t) + \gamma_{\rm MD}\dot{x}_{\rm MD}(t) + \omega_{\rm MD}^2 x_{\rm MD}(t) + g\dot{x}_{\rm exc}(t) = F(t) \tag{S.8a}$$

$$\ddot{x}_{\rm exc}(t) + \gamma_{\rm exc}\dot{x}_{\rm exc}(t) + \omega_{\rm exc}^2 x_{\rm exc}(t) - g\dot{x}_{\rm MD}(t) = 0. \tag{S.8b}$$

The extinction cross section is proportional to the work done by the force F driving the bound charges of the NP due to the incident electric field [4]

$$\sigma_{\rm ext} \propto \langle F(t)\dot{x}_{\rm MD}(t)\rangle \propto \omega\,{\rm Im}\left(\frac{\omega_{\rm exc}^2 - \omega^2 - i\gamma_{\rm exc}\omega}{(\omega_{\rm exc}^2 - \omega^2 - i\gamma_{\rm exc}\omega)(\omega_{\rm MD}^2 - \omega^2 - i\gamma_{\rm MD}\omega) - g^2\omega^2}\right), \tag{S.9}$$

where the angle brackets denote the average over a period of the oscillation. In Fig. S.3(b) we fit the extinction cross section spectrum of the coupled NP (black circles) with eqn (S.9) (red line) and find the coupling strength $\hbar g = 0.18$ eV. This value satisfies the strong coupling

criterion of eqn (S.7), $2\hbar g = 0.36$ eV $> \sqrt{(\hbar\gamma_{\rm exc})^2/2 + (\hbar\gamma_{\rm MD})^2/2} = 0.11$ eV, and therefore confirms that the system is strongly coupled.

Numerical simulations

The optical properties of the Ag NP helices (for geometrical details see main text) are simulated with commercial finite-element-method (FEM) software (Comsol Multiphysics 5.4). Each sphere is meshed with $15,000$ domain elements (distributed more densely near the gap between two NPs), while the excitonic matrix is meshed with $3,000$ elements. The simulation domain is a cube of side 400 nm, while perfectly-matched layers (PMLs) of thickness 400 nm are used on all sides of the domain. The domain is illuminated by a plane wave with x and y components of equal amplitude and phase difference $\pi/2$, and the full-field/scattered-field formulation is employed. Scattering and absorption cross sections are obtained by integrating the Poynting flux through the surface of the excitonic ellipsoidal matrix.

---

[1] C. F. Bohren and D. R. Huffman, *Absorption and Scattering of Light by Small Particles*, John Wiley and Sons, New York, 1983.

[2] G. Mie, *Ann. Phys.*, 1908, **330**, 377–445.

[3] P. Törmä and W. L. Barnes, *Rep. Prog. Phys.*, 2015, **78**, 013901.

[4] X. Wu, S. K. Gray and M. Pelton, *Opt. Express*, 2010, **18**, 23633–23645.